Determination of the intrinsic and the injection dependent charge carrier density in organic solar cells using the Suns-V_{OC} method

Sebastian Schiefer,[1,2] Birger Zimmermann,[1] and Uli Würfel[1,3,a)]
[1]*Fraunhofer Institute for Solar Energy Systems (ISE), Heidenhofstr. 2, 79110 Freiburg, Germany*
[2]*Department of Microsystems Engineering (IMTEK), University of Freiburg, Georges-Köhler-Allee 106, 79110 Freiburg, Germany*
[3]*Freiburg Materials Research Center (FMF), University of Freiburg, Stefan-Meier-Str. 21, 79104 Freiburg, Germany*

(Received 18 December 2013; accepted 9 January 2014; published online 27 January 2014)

A method is presented to calculate the intrinsic and injection dependent average charge carrier density from the transport resistance of an organic solar cell. The latter is determined using a combination of a Suns-V_{OC} and a current-voltage measurement under illumination which allows to split the total series resistance of the solar cell into an (ohmic) contribution of the circuitry and an injection dependent part which is caused by the transport of the charge carriers through the photoactive layer. In the derivation of the formula for the average charge carrier density, spatially homogeneous generation rate and gradients of the quasi Fermi levels as well as balanced mobilities had to be assumed. However, numerical simulations revealed that even for strongly inhomogeneous generation and unbalanced mobilities the results are reasonably accurate proving the practical applicability of the presented method. Using an inverted ITO-free P3HT:PCBM solar cell, we determined a value for the intrinsic charge carrier density of $n_i = 2.88 \times 10^{11}\,\mathrm{cm}^{-3}$ at $T = 300\,\mathrm{K}$ and for the average density of mobile charge carriers at "1 sun" under open circuit conditions we obtained $n_{av} = 3.2 \times 10^{16}\,\mathrm{cm}^{-3}$. © *2014 AIP Publishing LLC*.
[http://dx.doi.org/10.1063/1.4862960]

I. INTRODUCTION

Supplementary to experiments, the simulation of organic solar cells allows the evaluation of models, offers sound predictions, and improves the understanding of processes. The intrinsic charge carrier density n_i is an important material dependent parameter frequently used in simulation models.[1–8] In contrast to, e.g., crystalline silicon where the value of n_i has been determined very accurately,[9,10] it is rather unknown for the materials used in the photoactive layer of organic solar cells.

This work presents a new and simple method to determine the intrinsic charge carrier density of bulk heterojunction organic solar cells. At first, the charge carrier density dependent transport resistance is calculated from the combination of a Suns-V_{OC} curve and a current-voltage characteristics under illumination (Light JV). From this transport resistance, the injection-dependent density of mobile charge carriers is deduced which then allows the determination of the intrinsic charge carrier density n_i. In contrast to, e.g., silicon solar cells, the photoactive layer of BHJ-OSC is composed of an interpenetrating network of two materials, a donor and acceptor phase. For this reason, n_i is not the intrinsic density of one material, it denotes the charge carriers located in those energy levels where the excess electrons and holes under photovoltaic operation are transported and accumulated. These are the highest occupied molecular orbital (HOMO) of the donor for the holes and the lowest unoccupied molecular orbital (LUMO) of the acceptor for the electrons. The latter are often referred to as the transport levels of the effective semiconductor in BHJ-OSC. The quantity n_i is therefore characteristic for a specific donor/acceptor material combination.

II. EXPERIMENTAL ACCESS TO THE TRANSPORT RESISTANCE

It is possible to determine the injection dependent transport resistance of an (organic) solar cell by comparing a Light JV-curve with a Suns-V_{OC} measurement. The Suns-V_{OC} method was introduced by Sinton and Cuevas[11] and can be considered as a further development of the J_{SC}-V_{OC} measurements introduced by Wolf and Rauschenbach.[12] The method experienced several refinements[13,14] and developed to a widely used characterization method in the field of inorganic photovoltaics.[15–19] Recently, we showed the applicability of the Suns-V_{OC} method on organic solar cells.[20]

In a Suns-V_{OC} measurement, a solar cell is illuminated by a flash light which decays in intensity. During the variation of the light intensity over several orders of magnitudes, the open circuit voltage is continuously monitored. The illumination level can be associated with an implied current density and a pseudo JV-curve is obtained. This pseudo JV-curve is the curve the solar cell would have if there was no series resistance as there is no current flow during the Suns-V_{OC} measurement, see Ref. 20 for details.

The series resistance R_S can therefore be calculated as a function of current density J by subtracting the voltage of a pseudo JV-curve, i.e., V_{Suns} from the one of a Light JV-curve, denoted here as V_{JV}

a)Electronic address: uli.wuerfel@ise.fraunhofer.de

$$R_S(J) = \frac{V_{JV}(J) - V_{Suns}(J)}{J} = R_{circ} + R_{tr}(J). \quad (1)$$

As indicated in Eq. (1), the series resistance can be divided into two parts. One contribution is the (ohmic) series resistance related to the circuitry of the device, and the other one is the transport resistance caused by the motion of charge carriers through the photoactive layer. The transport resistance depends on the charge carrier densities; in contrast to most inorganic solar cells it can constitute a dominant contribution to the overall series resistance in organic solar cells due to the low charge carrier mobilities.[20] The series resistance caused by the circuitry R_{circ} can be estimated from the total series resistance at high current in forward direction. There, the charge carrier densities in the photoactive layer become very large and hence the corresponding transport resistance negligibly small. Once R_{circ} is known the transport resistance is obtained as a function of current density, $R_{tr}(J)$.

III. DERIVATION OF THE INJECTION DEPENDENT AND THE INTRINSIC CHARGE CARRIER DENSITY FROM $R_{tr}(J)$

This section introduces a method which allows to determine the average density of mobile charge carriers in the photoactive layer from the experimentally accessible transport resistance $R_{tr}(J)$. The latter is caused by the finite conductivities of electrons and holes

$$\sigma_{e/h} = q\,\mu_{e/h} n_{e/h} \quad (2)$$

with q being the elementary charge, $\mu_{e/h}$ the mobilities of electrons and holes, and $n_{e/h}$ their concentrations, respectively. The whole voltage drop $V_{tr} = J\,R_{tr}$ related to the transport of charge carriers through the photoactive layer is the difference between the voltages of the Suns-V_{OC} measurement and the Light JV-characteristics minus the voltage which drops over the outer circuitry and is obtained by a rearrangement of Eq. (1)

$$V_{tr} = J\,R_{tr} = V_{JV} - V_{Suns} - J\,R_{circ}. \quad (3)$$

Generally, the transport voltage does not drop homogeneously over the photoactive layer.

Fig. 1 shows a schematic sketch of the quasi Fermi levels of a solar cell under forward bias, i.e., $J > 0$. The gradients of the quasi Fermi levels provide the driving force for the transport of the charge carriers according to

$$J_{e/h} = \frac{\sigma_{e/h}}{q}\,\mathrm{grad}\,E_{F,e/h}. \quad (4)$$

For the given case of $J > 0$, electrons are injected through the electron contact and holes through the hole contact and they recombine at different positions x within the photoactive layer with each other. As a part of the outer voltage is required as driving force for the transport of the charge carriers, the separation of the quasi Fermi levels will be smaller than the outer voltage (corrected for the drop over R_{circ})

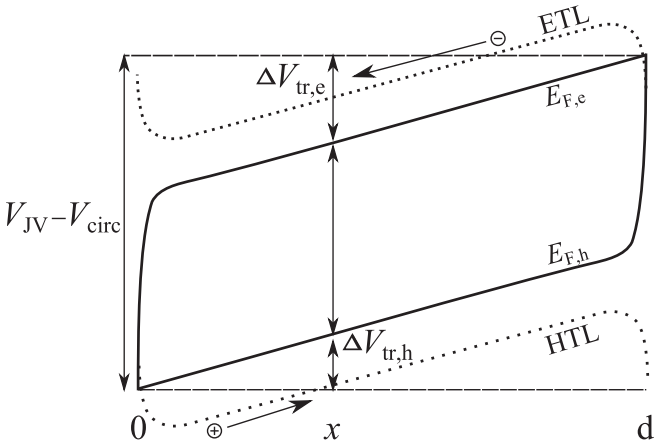

FIG. 1. Schematic of the quasi-Fermi levels of a solar cell under forward bias. The voltage at the contacts V_{JV} is composed of the voltage drop over the circuitry V_{circ}, the separation of the quasi-Fermi levels $E_{F,e}$–$E_{F,h}$ (which governs recombination) and voltage drops $\Delta V_{tr,e/h}$ caused by the transport of electrons and holes through the photoactive layer.

$$E_{F,e} - E_{F,h} < q(V_{JV} - V_{circ}). \quad (5)$$

In the case of $J < 0$, it is the other way round.

For the following, d shall be the thickness of the photoactive layer. The hole contact is located at $x = 0$ and the electron contact at $x = d$. For $J > 0$, the voltage $\Delta V_{tr,h}(x)$ which drops between the hole contact and a position x and the voltage $\Delta V_{tr,e}(x)$ which drops between x and the electron contact is due to the transport of holes and electrons, respectively, and given by

$$\Delta V_{tr,h}(x) = \int_0^x \frac{J_h(x')}{\sigma_h(x')}\,dx', \quad (6)$$

$$\Delta V_{tr,e}(x) = \int_x^d \frac{J_e(x')}{\sigma_e(x')}\,dx'. \quad (7)$$

The equations are also valid in the case of $J < 0$ (which changes the sign of $J_{e/h}$).

It is not possible in a straightforward manner to establish a simple and direct relationship between R_{tr} (J) and the average density of mobile charge carriers n_{av} inside the photoactive layer. The reason is that the current densities as well as the conductivities of electrons and holes in Eqs. (6) and (7) are unknown functions of the position within the photoactive layer. Although the overall voltage drop V_{tr} can be determined according to Eq. (3), its distribution within the photoactive layer remains unknown. This problem will be investigated in greater detail in the supplementary information.[21] Here, the aim is to derive an analytical formula for n_{av} as a function of the experimentally accessible quantity $R_{tr}(J)$.

For this reason, several assumptions are used in the following. Afterward, results from numerical simulations are presented which evaluate the usefulness of this approach. The assumptions are

1) $\frac{J_e(x)}{\sigma_e(x)} = \frac{J_h(x)}{\sigma_h(x)} = \mathrm{grad}\,E_{F,e/h} = \mathrm{const.}$

2) $\mu_e = \mu_h = \mu$

From the first assumption follows:

$$\Delta V_{tr,h}(x) + \Delta V_{tr,e}(x) = \text{const.} = V_{tr}$$

$$V_{tr} = \frac{J_h(x')}{\sigma_h(x')}\int_0^x dx' + \frac{J_e(x')}{\sigma_e(x')}\int_x^d dx' = \left(\frac{J_h}{\sigma_h} + \frac{J_e}{\sigma_e}\right)d. \quad (8)$$

Note that the first assumption implies that there is no surface recombination and the recombination in the bulk is homogeneous. Combining both assumptions leads to

$$\frac{J_h(x')}{n_h(x')} = \frac{J_e(x')}{n_e(x')} = \text{const.} \quad (9)$$

Hence, these quantities can be replaced by their average values

$$V_{tr} = \frac{d}{q\,\mu}\left(\frac{\overline{J_h}}{\overline{n_h}} + \frac{\overline{J_e}}{\overline{n_e}}\right). \quad (10)$$

Since $\overline{J_h} = \overline{J_e} = J/2$, it is also $\overline{n_e} = \overline{n_h} = n_{av}$ and therefore we obtain

$$V_{tr} = \frac{J\,d}{2\,q\,\mu\,n_{av}}. \quad (11)$$

Using $V_{tr} = J\,R_{tr}$, it follows the desired expression for the average density of mobile charge carriers n_{av}

$$n_{av}(J) = \frac{d}{2\,q\,\mu\,R_{tr}(J)}. \quad (12)$$

The intrinsic charge carrier concentration n_i can then be determined using the following relation:

$$n_e\,n_h = n_i^2 \exp\left(\frac{E_{F,e} - E_{F,h}}{kT}\right). \quad (13)$$

Therein, k is the Boltzmann-constant and T the temperature. As there is no surface recombination, the separation of the quasi Fermi energies can be replaced by the voltage V_{Suns} recorded between the terminals during a Suns-V_{OC} measurement. This leads to the expression for the intrinsic charge carrier density n_i

$$n_i = \frac{d}{R_{tr}(J)\,2\,q\,\mu\exp[q\,V_{Suns}/(2kT)]}. \quad (14)$$

As already mentioned above, the charge carriers in Eq. (12) are only those which are mobile and thus take part in the transport. The potential contribution of trapped charge carriers to the overall recombination is correctly accounted for as the voltages in Eq. (3) are measured quantities.

IV. EVALUATION OF THE ACCURACY OF EQ. (12)

The above mentioned assumptions Eq. (12) is based on, i.e., constant gradients of the quasi Fermi energies throughout the photoactive layer and balanced mobilities, are of course not strictly fulfilled in real devices. Therefore, it has to be carefully evaluated in how far Eq. (12) can serve as a reasonably exact approximation of the charge carrier density in the photoactive layer of organic solar cells. An appropriate way to do so is by means of numerical simulations as it enables comparing the value resulting from the application of Eq. (12) with the real spatial average of the charge carrier concentrations extracted from the simulation data

$$\overline{n_{e/h}} = \sqrt{\frac{1}{d}\int_0^d n_e(x)\,n_h(x)dx}. \quad (15)$$

We investigated the following three scenarios:

i) homogeneous generation and balanced mobilities
ii) inhomogeneous generation and balanced mobilities
iii) homogeneous generation and unbalanced mobilities

The simulations are based on a so-called effective semiconductor model where the electron transport level corresponds to the LUMO of the acceptor phase and the hole transport level to the HOMO of the donor phase. Details of the model can be found in Ref. 3. The simulations were carried out with the commercial semiconductor simulation tool TCAD Sentaurus from Synopsys Inc.[22] The work functions were chosen to be $W_{F,e} - E_{LUMO} = E_{HOMO} - W_{F,h} = 0.2\,\text{eV}$, which ensures a negligible rate of surface recombination. The thickness of the photoactive layer was in all cases $d = 220\,\text{nm}$. If not otherwise mentioned, the mobility of electrons and holes was $\mu_{e/h} = 3.5 \times 10^{-4}\,\text{cm}^2(\text{V s})^{-1}$. The generation rate for (i) and (iii) was spatially homogeneous with a value of $G = 2.75 \times 10^{21}\,\text{cm}^{-3}\text{s}^{-1}$ which corresponds to a maximum short circuit current density of $J_{SC,max} = -q\int_0^d G(x)\,dx \approx -11\,\text{mA/cm}^2$.

A Light JV-curve and, instead of a transient Suns-V_{OC} curve, a steady-state J_{SC}–V_{OC} curve[12] was simulated which delivers exactly the same information. First, the value of R_{tr} was determined. No series resistance of the circuitry was considered in the numerical simulations, i.e., $R_{circ} \equiv 0$. Then, using Eq. (12), the value of the average charge carrier density n_{av} as a function of illumination intensity was calculated. Finally, the value of n_{av} was compared to $\overline{n_{e/h}}$ according to Eq. (15).

A. Homogeneous generation and balanced mobilities

The black curves in Fig. 2 show the results for this scenario. The charge carrier density depicted with the solid line was calculated using the transport resistance and the data for the dashed line were extracted directly from the spatially dependent charge carrier density according to Eq. (15).

It can be seen that the values calculated according to Eq. (12) are lower than the directly extracted ones for intensities higher than one sun—although the differences are rather small. The inset is a magnification of the curves around an intensity of "1 sun" and it shows that the curves intercept at roughly "0.75 suns." To explain this, it has to be

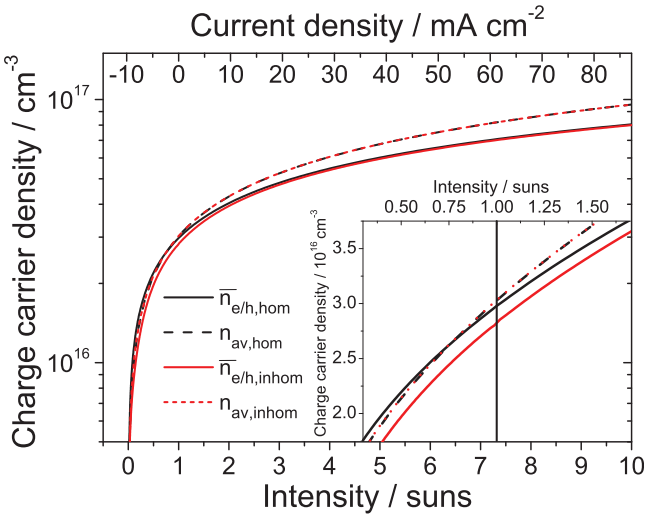

FIG. 2. Comparison of the charge carrier density determined via the transport resistance (dashed lines) with the spatial average charge carrier density directly extracted from the simulation data (solid line). The black lines correspond to a homogeneous generation, whereas the red lines were calculated using a strongly inhomogeneous generation profile (see text).

taken into account that Eq. (12) assumes a constant and equal value for the electron and hole concentrations and hence in the case of constant and balanced mobilities also constant and equally large conductivities. In contrast, in the numerical simulations, the distributions of the conductivities are strongly inhomogeneous. This gives rise to inhomogeneities in the corresponding current densities and the recombination rate, in contrast to what had to be assumed in the former section. This finally leads to the small but notable deviations of the charge carrier density determined via the transport resistance (Eq. (12)) and the average charge carrier concentration determined via Eq. (15).

These results prove that for a spatially homogeneous generation rate and balanced mobilities of electrons and holes, the average charge carrier density can in good approximation be determined with Eq. (12). However, as these conditions are typically not fulfilled, it has to be found out if our approach can also be applied to more realistic scenarios. Therefore, two practically more important cases have been investigated and another two sets of calculations were performed.

B. Inhomogeneous generation and balanced mobilities

This was performed by adjusting an exponentially decaying generation rate to the same total amount of generated charge carriers as the previously used homogeneous one. This profile decreased from its initial value at the hole contact to ca. 11% of this value at the position of the electron contact. It should be noted that this profile can be safely considered as an upper limit regarding the non-homogeneity of a generation profile for P3HT:PCBM solar cells under white light. The red curves in Fig. 2 show the results again according to Eq. (12) (solid line) and Eq. (15) (dashed line). In this case, the two curves do not intercept, the solid line (from the transport resistance) underestimates the "real" value. However, the deviation is again rather small (below 10%) and hence confirms the applicability also for this case.

C. Homogeneous generation and unbalanced mobilities

The last variation was done to investigate the influence of unbalanced mobilities. We changed the value of the electron mobility to $\mu_e = 10^{-3}\,\mathrm{cm^2(Vs)^{-1}}$ leaving the hole mobility unchanged at $\mu_h = 3.5 \times 10^{-4}\,\mathrm{cm^2(Vs)^{-1}}$. The results are shown in Fig. 3. It can be seen that for this case the deviation is larger when using either the (higher) electron mobility (red curve) or the (lower) hole mobility (blue curve) in Eq. (12). However, when using the geometric average of the mobility $\mu_{e/h} = \sqrt{\mu_e\,\mu_h}$ (black solid curve), the average charge carrier density can again be approximated within less than 10%.

These two examples show that the presented method can be applied to determine the average charge carrier concentration in the photoactive layer of organic solar cells quite accurately also for realistic scenarios. In the next section, this procedure will be applied to a bulk-heterojunction organic solar cell based on P3HT:PCBM.

V. EXPERIMENTAL DETERMINATION OF THE INJECTION DEPENDENT AND INTRINSIC CHARGE CARRIER DENSITY OF A P3HT:PCBM SOLAR CELL

We have applied this method to determine n_{av} and n_i of ITO-free inverted organic solar cells.[23–26] A metal grid and highly conductive PEDOT:PSS is used as a hole contact. The photoactive layer consists of a blend of P3HT and PCBM. 5 nm chromium and 100 nm aluminum followed by another 5 nm chromium were thermally evaporated on a cleaned glass substrate. On top of this electron contact, a solution was spin coated consisting of 20 mg of P3HT 4002-E from Rieke metals and 15 mg of PCBM 99% from Solenne per milliliter ortho-xylene. The rotation speed was set to

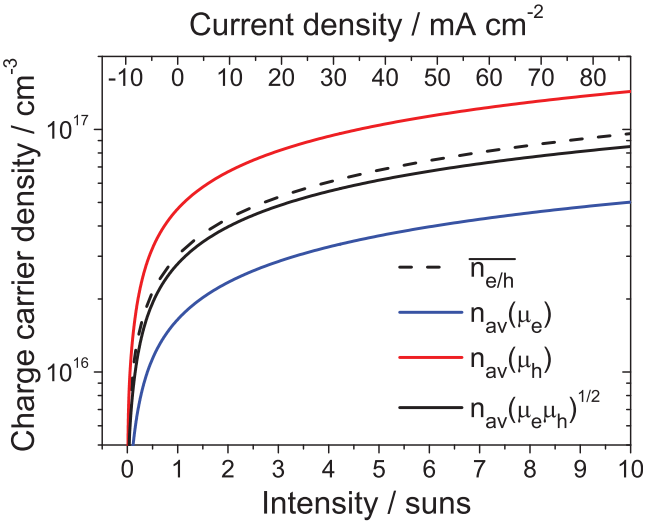

FIG. 3. The average charge carrier density calculated with Eq. (12) using the lower mobility of the holes (red), the higher mobility of the electrons (blue), or the geometrical average of both mobilities (solid black) in comparison to the spatial average charge carrier density determined with Eq. (15).

500 rpm which corresponds to an approximate layer thickness of 220 nm. On top, an approximately 85 nm thick layer of PEDOT:PSS (Heraeus-Clevios F010) was spin-coated with a rotation speed of 3000 rpm. A 100 nm thick silver grid was evaporated in the end and the cell was finally annealed at 120 °C for 10 min.

The Light JV-curve at "1 sun" was measured with a Keithley 2400 Sourcemeter and a Steuernagel SolarCellTest 575 sun-simulator. The data were mismatched to simulate AM1.5 G conditions (1000 W/m^2). For the Suns-V_{OC} measurement, a WCT-120 stage from Sinton Instruments was used. The results were also mismatched to the relative spectral distribution of the AM1.5 G spectrum (the intensity varied of course).

The Light JV-curve and the pseudo JV-curve obtained from the Suns-V_{OC} data are both depicted in Fig. 4.

As the result for n_{av} is reciprocally proportional to the charge carrier mobility, the uncertainty in the value of the latter is reflected directly in the uncertainty of n_{av} and thus also of n_i. For sake of simplicity, the same value as for the numerical device simulations was used for the charge carrier mobilities, i.e., $\mu_{e/h} = 3.5 \times 10^{-4}\,\mathrm{cm^2(Vs)^{-1}}$. Note that this value is in the range of experimentally detected mobilities of P3HT in our laboratory from charge extraction by linearly increasing voltage (CELIV) measurements and from the space charge limited current (SCLC) of hole-only devices. The value is in accordance with results from literature.[27–30] It has to be stated that the results of these measurements can be influenced by traps[31] as well as by the actual morphology of the photoactive layer. Both depend on the processing conditions such as choice of solvent, annealing time, and temperature.

Using Eq. (1), the injection dependent transport resistance was determined with the series resistance of the circuitry R_{circ} being approximately 2 Ωcm^2. The charge carrier density calculated from the transport resistance according to Eq. (12) is plotted in Fig. 5. It has a pole at an intensity of "1 sun" as there is no current flowing, therefore extrapolation was used to determine the corresponding value $n_{av} = 3.2 \times 10^{16}\,\mathrm{cm^{-3}}$

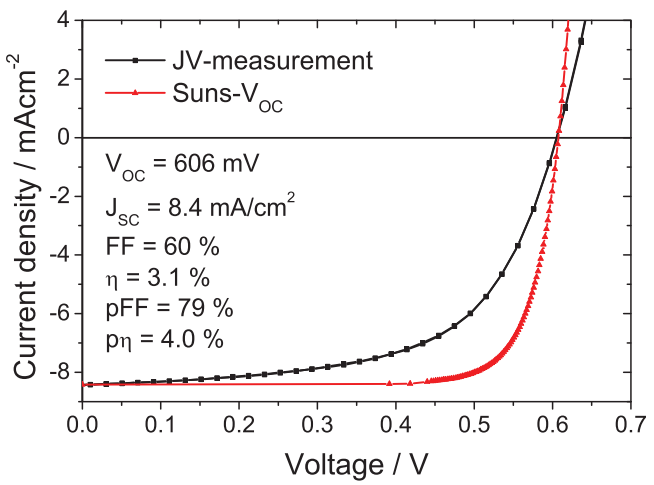

FIG. 4. JV-curve measured at standard conditions (simulated AM1.5 G, i.e., "1 sun") and a pseudo JV-curve determined by the Suns-V_{OC} method from an inverted ITO-free organic solar cell based on a P3HT:PCBM blend.

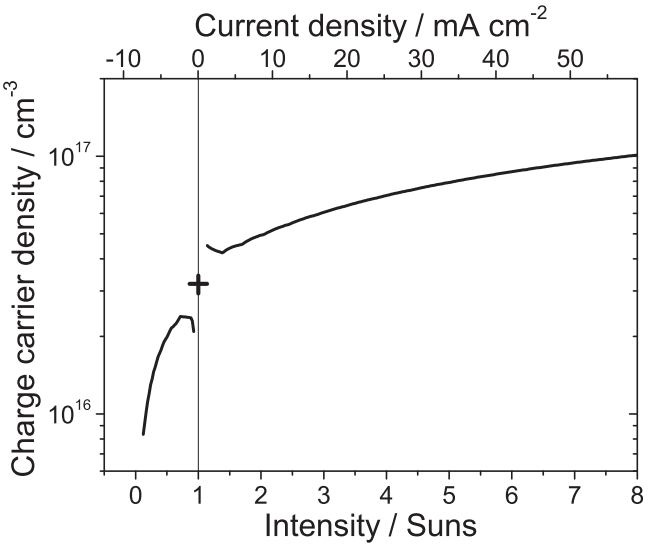

FIG. 5. Charge carrier density calculated from the transport resistance which was deduced from the comparison of a Suns-V_{OC} and a JV-measurement at "1 sun." The charge carrier density at "1 sun" was extrapolated from the rest of the curve.

of mobile charge carriers (marked with a cross). From this, a value of $n_i = 2.4 \times 10^{11}\,\mathrm{cm^{-3}}$ at the temperature of the experiment $T = 297.6\,\mathrm{K}$ was derived. In order to compare it more easily with the simulations, we calculated the value $n_i(T = 300\,\mathrm{K}) = 2.88 \times 10^{11}\,\mathrm{cm^{-3}}$ neglecting the temperature dependence of the band gap energy.

This value is identical to the one from our simulation model $(n_{i,sim} = 2.88 \times 10^{11}\,\mathrm{cm^{-3}})$ which shows that the parameters used in our simulations are very reasonable.

Table I shows a collection of values for n_i taken from literature reporting on the simulation of P3HT:PCBM solar cells. It can be seen that there is quite a large variation for n_i spanning more than two orders of magnitude in the different publications. The reason is that it is not possible to determine its value from simulations by adjusting, e.g., the open circuit voltage. Even if the generation rate is known, there is still a considerable uncertainty as the density of states as well as the recombination coefficient are tunable parameters which influence the results.

The great advantage of the method applied in this work is that the average and also the intrinsic charge carrier density are derived directly from the experimentally accessible transport resistance. The latter is only a function of charge

TABLE I. Intrinsic charge carrier density calculated from the bandgap and the effective density of states taken from different publications for P3HT:PCBM.

	Bandgap E_g (eV)	Effective density of states $N_{C,V}$ (cm^{-3})	Intrinsic charge carrier density n_i at $T = 300$ K (cm^{-3})
Schafferhans *et al.*[32]	1.3	8×10^{19}	9.62×10^{8}
Deibel *et al.*[7]	1.35	10^{21}	4.57×10^{9}
Garcia-Belmonte *et al.*[33]	1.2	10^{21}	8.32×10^{10}
MacKenzie *et al.*[34]	1.1	1.9×10^{20}	1.09×10^{11}
Stelzl *et al.*,[3] Glatthaar *et al.*,[35] and this work	1.1	5×10^{20}	2.88×10^{11}

carrier densities and mobilities and does therefore not depend neither on the density of states nor on the recombination coefficient. This way, our method can significantly narrow down the range for n_i.

VI. CONCLUSIONS

A method was presented that allows to determine the injection dependent as well as the intrinsic charge carrier density of bulk-heterojunction organic solar cells directly from the experimental data of a current-voltage characteristics under illumination and a Suns-V_{OC} measurement. To derive the corresponding formula, spatially homogeneous generation and gradients of the quasi Fermi energies as well as balanced charge carrier mobilities had to be assumed. To evaluate the accuracy of this approach, numerical simulations were performed to compare the values based on the presented method with the ones extracted from simulation results. It turned out that our approach delivers reasonably good approximations also for realistic scenarios such as inhomogeneous generation and unbalanced charge carrier mobilities. Applying the procedure to an ITO-free inverted P3HT:PCBM cell, we found a value of $n_{av} = 3.2 \times 10^{16}\,\mathrm{cm}^{-3}$ for the density of mobile charge carriers under open circuit conditions at an illumination intensity of "1 sun". From this, the intrinsic charge carrier density was determined to be $n_i(T = 300\,\mathrm{K}) = 2.88 \times 10^{11}\,\mathrm{cm}^{-3}$. To the best of our knowledge, this is the first experimentally detected value for n_i of P3HT:PCBM and constitutes thus a substantial step toward a more precise description of the operational principles of organic solar cells.

ACKNOWLEDGMENTS

This work was partially funded by the German Ministry of Education and Science under Contract No. 03EK3505H. U.W. acknowledges support from the DFG in the framework of SPP1355.

[1]S. Zhou, J. Sun, C. Zhou, and Z. Deng, "Comparison of recombination models in organic bulk heterojunction solar cells," Physica B **415**, 28–33 (2013).
[2]W. Tress, K. Leo, and M. Riede, "Optimum mobility, contact properties, and open-circuit voltage of organic solar cells: A drift-diffusion simulation study," Phys. Rev. B **85**, 155201 (2012).
[3]F. F. Stelzl and U. Würfel, "Modeling the influence of doping on the performance of bulk heterojunction organic solar cells: One-dimensional effective semiconductor versus two-dimensional donor/acceptor model," Phys. Rev. B **86**, 075315 (2012).
[4]L. M. Andersson, C. Müller, B. H. Badada, F. Zhang, U. Würfel, and O. Inganäs, "Mobility and fill factor correlation in geminate recombination limited solar cells," J. Appl. Phys. **110**, 024509-7 (2011).
[5]V. A. Trukhanov, V. V. Bruevich, and D. Y. Paraschuk, "Effect of doping on performance of organic solar cells," Phys. Rev. B **84**, 205318 (2011).
[6]A. Wagenpfahl, D. Rauh, M. Binder, C. Deibel, and V. Dyakonov, "S-shaped current-voltage characteristics of organic solar devices," Phys. Rev. B **82**, 115306 (2010).
[7]C. Deibel, A. Wagenpfahl, and V. Dyakonov, "Influence of charge carrier mobility on the performance of organic solar cells," Phys. Status Solidi (RRL) **2**, 175–177 (2008).
[8]M. M. Mandoc, L. J. A. Koster, and P. W. M. Blom, "Optimum charge carrier mobility in organic solar cells," Appl. Phys. Lett. **90**, 133504 (2007).
[9]P. P. Altermatt, A. Schenk, F. Geelhaar, and G. Heiser, "Reassessment of the intrinsic carrier density in crystalline silicon in view of band-gap narrowing," J. Appl. Phys. **93**, 1598–1604 (2003).
[10]A. B. Sproul, M. A. Green, and J. Zhao, "Improved value for the silicon intrinsic carrier concentration at 300 k," Appl. Phys. Lett. **57**, 255–257 (1990).
[11]R. Sinton and A. Cuevas, "A quasi-steady-state open-circuit voltage method for solar cell characterization," in *Proceedings of the 16th European Photovoltaic Solar Energy Conference, Glasgow, UK* (2000), pp. 1152–1155.
[12]M. Wolf and H. Rauschenbach, "Series resistance effects on solar cell measurements," Adv. Energy Convers. **3**, 455–479 (1963).
[13]M. J. Kerr, A. Cuevas, and R. A. Sinton, "Generalized analysis of quasi-steady-state and transient decay open circuit voltage measurements," J. Appl. Phys. **91**, 399–404 (2002).
[14]A. Cuevas and F. Recart, "Capacitive effects in quasi-steady-state voltage and lifetime measurements of silicon devices," J. Appl. Phys. **98**, 074507 (2005).
[15]D. Pysch, A. Mette, and S. Glunz, "A review and comparison of different methods to determine the series resistance of solar cells," Sol. Energy Mater. Sol. Cells **91**, 1698–1706 (2007).
[16]S. W. Glunz, J. Nekarda, H. Mäckel, and A. Cuevas, "Analyzing back contacts of silicon solar cells by suns-voc-measurements at high illumination densities," in Proceedings of the 22nd European Photovoltaic Solar Energy Conference Milan, Italy, 2007.
[17]A. Cuevas and R. A. Sinton, "Detailed modelling of the effective minority carrier lifetime and the open-circuit voltage of silicon solar cells," in *Proceedings of the 22nd European Photovoltaic Solar Energy Conference, Milan, Italy* (2007), pp. 38–43.
[18]K. Wilson, D. D. Ceuster, and R. A. Sinton, "Measuring the effect of cell mismatch on module output," in *Conference Record of the 2006 IEEE 4th World Conference on Photovoltaic Energy Conversion* (2006), Vol. 1, pp. 916–919.
[19]J. Schmidt, A. Cuevas, S. Rein, and S. W. Glunz, "Impact of light-induced recombination centres on the current-voltage characteristic of czochralski silicon solar cells," Prog. Photovoltaics **9**, 249–255 (2001).
[20]S. Schiefer, B. Zimmermann, S. Glunz, and U. Würfel, "Applicability of the suns-voc method on organic solar cells," IEEE J. Photovolt. **4**, 271–277 (2014).
[21]See supplementary material at http://dx.doi.org/10.1063/1.4862960 for a detailed discussion of the voltage drops occurring due to the transport of electrons and holes.
[22]Synopsys, Tcad sentaurus: Sentaurus Device User Guide, Release h-2013.03, see www.synopsys.com, 2013.
[23]B. Zimmermann, H.-F. Schleiermacher, M. Niggemann, and U. Würfel, "ITO-free flexible inverted organic solar cell modules with high fill factor prepared by slot die coating," Sol. Energy Mater. Sol. Cells **95**, 1587–1589 (2011).
[24]B. Zimmermann, U. Würfel, and M. Niggemann, "Longterm stability of efficient inverted P3HT:PCBM solar cells," Sol. Energy Mater. Sol. Cells **93**, 491–496 (2009).
[25]B. Zimmermann, M. Glatthaar, M. Niggemann, M. K. Riede, T. Ziegler, and A. Gombert, "Organic solar cells with inverted layer sequence incorporating optical spacers—Simulation and experiment," Proc. SPIE **6197**, 61970G1-6 (2006).
[26]M. Glatthaar, M. Niggemann, B. Zimmermann, P. Lewer, M. Riede, A. Hinsch, and J. Luther, "Organic solar cells using inverted layer sequence," Thin Solid Films **491**, 298–300 (2005).
[27]A. Mozer, N. Sariciftci, A. Pivrikas, R. Österbacka, G. Juska, L. Brassat, and H. Bässler, "Charge carrier mobility in regioregular poly(3-hexylthiophene) probed by transient conductivity techniques: A comparative study," Phys. Rev. B **71**, 035214 (2005).
[28]S. Choulis, Y. Kim, J. Nelson, D. Bradley, M. Giles, M. Shkunov, and I. McCulloch, "High ambipolar and balanced carrier mobility in regioregular poly(3-hexylthiophene)," Appl. Phys. Lett. **85**, 3890–3892 (2004).
[29]A. M. Ballantyne, L. Chen, J. Dane, T. Hammant, F. M. Braun, M. Heeney, W. Duffy, I. McCulloch, D. D. C. Bradley, and J. Nelson, "The effect of poly(3-hexylthiophene) molecular weight on charge transport and the performance of polymer:fullerene solar cells," Adv. Funct. Mater. **18**, 2373–2380 (2008).
[30]L. J. A. Koster, V. D. Mihailetchi, H. Xie, and P. W. M. Blom, "Origin of the light intensity dependence of the short-circuit current of polymer/fullerene solar cells," Appl. Phys. Lett. **87**, 203502 (2005).

[31]R. Hanfland, M. A. Fischer, W. Brutting, U. Würfel, and R. C. I. MacKenzie, "The physical meaning of charge extraction by linearly increasing voltage transients from organic solar cells," Appl. Phys. Lett. **103**, 063904 (2013).
[32]J. Schafferhans, A. Baumann, A. Wagenpfahl, C. Deibel, and V. Dyakonov, "Oxygen doping of P3HT:PCBM blends: Influence on trap states, charge carrier mobility and solar cell performance," Org. Electron. **11**, 1693–1700 (2010).
[33]G. Garcia-Belmonte, P. P. Boix, J. Bisquert, M. Sessolo, and H. J. Bolink, "Simultaneous determination of carrier lifetime and electron density-of-states in P3HT:PCBM organic solar cells under illumination by impedance spectroscopy," Sol. Energy Mater. Sol. Cells **94**, 366–375 (2010).
[34]R. C. I. MacKenzie, C. G. Shuttle, M. L. Chabinyc, and J. Nelson, "Extracting microscopic device parameters from transient photocurrent measurements of p3ht:pcbm solar cells," Adv. Energy Mater. **2**, 662–669 (2012).
[35]M. Glatthaar, M. Riede, N. Keegan, K. Sylvester-Hvid, B. Zimmermann, M. Niggemann, A. Hinsch, and A. Gombert, "Efficiency limiting factors of organic bulk heterojunction solar cells identified by electrical impedance spectroscopy," Sol. Energy Mater. Sol. Cells **91**, 390–393 (2007).